

# Electrically switchable achromatic liquid crystal polarization gratings on reflective substrates

Chulwoo Oh and Michael J. Escuti

North Carolina State Univ, Dept Electrical & Computer Engineering, Raleigh, NC (USA)

## ABSTRACT

We have experimentally demonstrated broadband light modulation by achromatic liquid crystal (LC) polarization gratings (PGs), which manifest polarization-independent modulation with high efficiencies ( $\geq 95\%$ ). Recently, we introduced achromatic PGs with a unique double-layer, reversed-twist structure as efficient, broadband polarizing beamsplitters. We now report on our successful implementation of electrically switchable achromatic LCPGs on a reflective substrate. To pattern a spiraling, periodically varying LC profile, we utilize polarization holography and photoalignment techniques. Use of reflective substrates enables the same retardation compensation of double-layer achromatic PGs. In addition, perhaps most importantly, the single cell structure allows the electro-optical switching/modulation by applying an electric field across the cell. The achromatic LCPG sample shows steeper voltage responses and less spectral shifts while operating in grayscale with respect to previously reported LCPGs. Relatively faster switching times ( $\sim 6$  msec for  $3\ \mu\text{m}$ -thickness) were measured compared to a conventional LCPG with the same thickness ( $\sim 10$  msec). Interesting electro-optical behaviors were also observed including zero-voltage threshold and a hysteresis in the voltage response.

**Keywords:** achromatic diffraction, polarization grating, liquid crystals, holography, polarizing beamsplitter, light modulator

## 1. INTRODUCTION

Efficient light modulation is essential for displays, light shutters, optical data storages, optical communication, and many other applications. Recent advances in liquid crystal polarization gratings (LCPGs)<sup>1-5</sup> suggest they have strong potential as polarization independent light modulators, exhibiting a high contrast ratio and a high diffraction efficiency up to  $\sim 100\%$ . Since LCPGs can modulate unpolarized light and remove polarizers from conventional LC switching devices, the overall efficiency/throughput can be doubled, especially suitable for portable displays and pocket-size projectors. There are a number of alternative approaches for polarization-independent light modulators, including LC-gels,<sup>6</sup> PDLCs,<sup>7</sup> H-PDLCs,<sup>8</sup> and binary LC gratings.<sup>9</sup> Most of them, however, suffer from inherent scattering, low contrast ratios, and limited peak efficiencies. While conventional LCPGs avoid or overcome these disadvantages, their reflectance/transmittance properties are nevertheless not completely insensitive to wavelength, as most retardation-based LC elements (e.g. homogeneous LC cell between crossed-polarizers). Although this wavelength sensitivity is usual in LC devices, achromatic diffraction is much more attractive for applications where a broadband light source is used.<sup>10-12</sup>

The majority of LC light modulators operate by controlling the direction of polarization of the light passing through it, via the birefringence and perhaps twist of the LC layer. Since the optical properties of such LC modulators are very sensitive to polarizations of incident light, practically all of them require a single, known input polarization, usually achieved with a polarizer at the device input that reduces the light efficiency by more than 50%. In addition, some of these have dependence on wavelengths due to the material dispersion (e.g. most easily observed in tunable LC waveplates as well as vertically-aligned-nematic (VAN) mode displays). The wavelength sensitivity may lead to spectral shifts in the grayscale properties with applied RMS voltages. There are a number of ways to compensate this chromatic dependence. The most successful approach is through retardation compensation, and the case most relevant to this work is double-layered super-twisted LC devices,<sup>13</sup> which is possible by balancing the dispersion of retardation and optical activity induced by the twist.

---

Correspondence should be sent to: mjescuti@ncsu.edu, Telephone: +1 919 513 7363

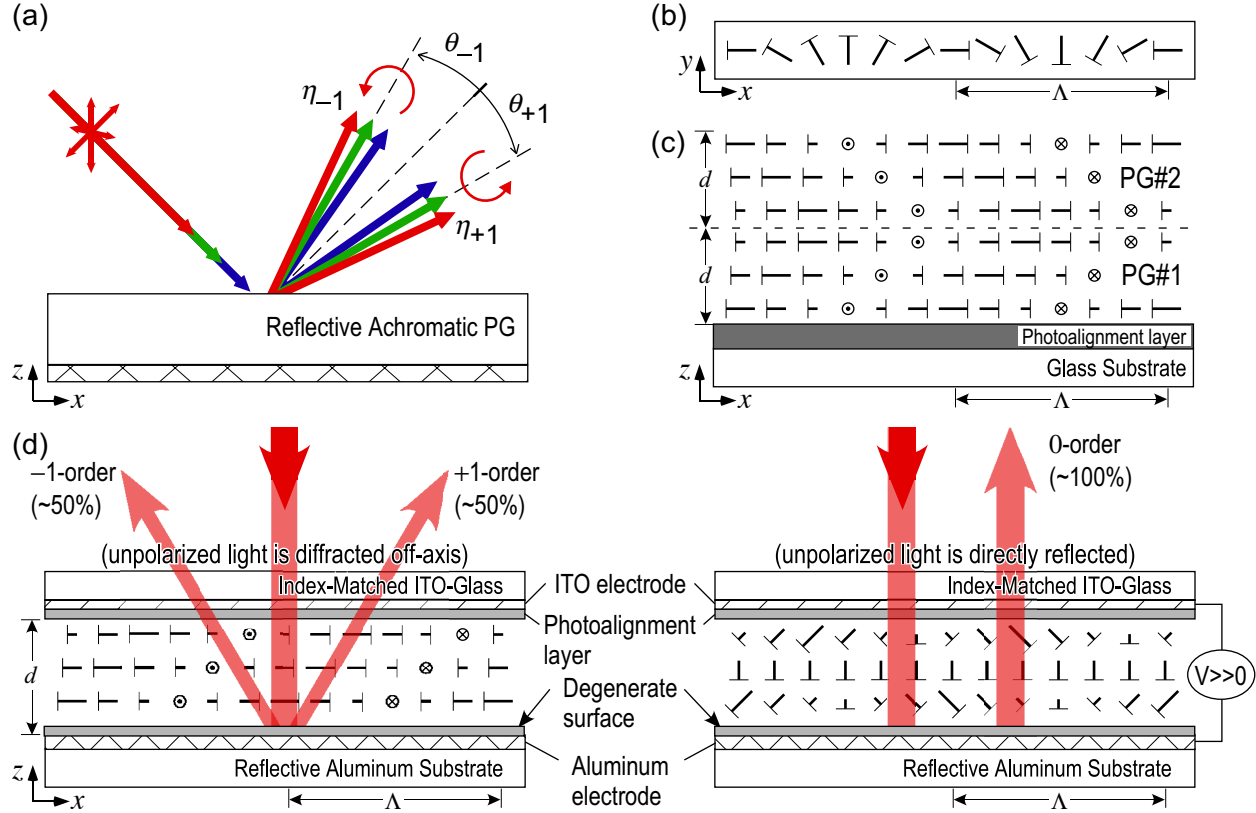


Figure 1. Basic structure and light switching of a reflective achromatic LCPG: (b) diffraction from reflective achromatic PGs; (b) a spiraling, periodically varying anisotropy profile of Circular PGs; (c) a schematic view of transmissive achromatic PG; (d) a reflective achromatic LCPG and its electro-optical switching.

We here report on our recent successful demonstrations of electrically switchable achromatic LCPGs on reflective substrates, which shows polarization-independent modulation as well as very high efficiencies (up to  $\sim 100\%$ ). We already demonstrated transmissive achromatic PGs formed as polymer films of reactive mesogens.<sup>14, 15</sup> Since the self-compensated structure for achromatic PGs requires two twisted layers with opposite twist senses (i.e., left- or right-handednesses) as shown in Fig. 1(c), two separate LCPG cells can be assembled. However, a double cell structure may cause a number of problems, including high driving voltages and image parallax due to the middle substrate. We have found a unique way to implement achromatic LCPGs as a single-cell reflective LC device utilizing the antisymmetric (or chiral) nature of twist upon reflection (i.e., light experiences left- and right-handed twist before and after reflection, respectively). We implemented achromatic LCPG samples showing broadband diffraction with high efficiencies ( $\geq 95\%$ ) over the visible wavelengths (450 nm to 650 nm). We will show electro-optical properties of achromatic LCPGs including voltage responses, switching times, and diffraction spectra in grayscale operation. We will also discuss the effect of the presence of twist on the electro-optical properties – fast switching and hysteresis in the voltage response.

## 2. BACKGROUND

The most-studied PGs<sup>16–19</sup> have its anisotropic profile consisting of a spiraling, constant magnitude, linear birefringence but constant along the thickness (i.e.,  $\mathbf{n}(x) = [\sin(\pi x/\Lambda), \cos(\pi x/\Lambda), 0]$ , where  $\mathbf{n}$  is a unity vector, also known as a nematic director for LCs, to describe the orientation of the linear birefringence and  $\Lambda$  is the effective optical period) as shown in Fig. 1(b), which are also called Circular PGs<sup>20</sup> due to their sensitivity of diffraction to the circular polarization. The ideal diffraction efficiency at normal incidence can be derived with

Jones calculus<sup>21</sup> (a reformulation of Refs.<sup>16,19</sup>):

$$\eta_0 = \cos^2 \left( \frac{\pi \Delta n d}{\lambda} \right) \quad (1a)$$

$$\eta_{\pm 1} = \left( \frac{1 \mp S'_3}{2} \right) \sin^2 \left( \frac{\pi \Delta n d}{\lambda} \right), \quad (1b)$$

where  $\eta_m$  is the diffraction efficiency of the  $m^{\text{th}}$ -order,  $\lambda$  is the vacuum wavelength of incident light,  $\Delta n$  is the linear birefringence,  $d$  is the grating thickness, and  $S'_3 = S_3/S_0$  is the normalized Stokes parameter<sup>22</sup> corresponding to ellipticity of the incident polarization. Circular PGs manifest a unique combination of optical properties including only three orders (0 and  $\pm 1$ ) possible, up to 100% efficiency into a single order, orthogonal circular polarizations (left- and right-handed) of the first orders. Note that the diffraction behavior of Circular PGs depends modestly on the wavelength (through  $\Delta n d/\lambda$  in Eqs. 1).

We introduced achromatic polarization gratings<sup>15</sup> with low-angle twist ( $\sim 70^\circ$ ) as shown in Fig. 1(c). For the achromatic PGs, the anisotropy pattern varies also with the thickness (i.e., twist for LCs), not only in the plane. The achromatic diffraction can be achieved by the self-retardation compensation of the double-layer reversed-twist structure with the same angle but the opposite sense of twist. Similar achromatic effect by twist is well known in super-twisted nematic LC displays. We derived the analytical expressions for diffraction properties including field vectors and efficiencies using the Jones matrix analysis and experimentally demonstrated achromatic PGs as thin transparent polymer films of reactive mesogen (polymerizable LC).<sup>23,24</sup> The maximum bandwidth for a high efficiency ( $\geq 99\%$ ) was obtained over the entire visible wavelengths (i.e., from 450 nm to 650 nm).

The achromatic PG comprises two antisymmetric chiral Circular PG layers with opposite twist senses, where the nematic director  $\mathbf{n}$  follows:

$$\mathbf{n}(x, z) = [\cos \phi(x, z), \sin \phi(x, z), 0] \quad (2a)$$

$$\phi(x, z) = \begin{cases} \pi x/\Lambda + \Phi z/d & \text{if } 0 \leq z \leq d \\ \pi x/\Lambda - \Phi z/d + 2\Phi & \text{if } d < z \leq 2d \end{cases} \quad (2b)$$

where  $\phi$  is the azimuth angle of the director field,  $\Lambda$  is the grating period,  $d$  is the thickness, and  $\Phi$  is the twist angle of each chiral layer. Fig. 1(c) illustrates this profile. Nematic LC materials and photoalignment techniques are ideal to create this anisotropic pattern since their orientation can be initially established by surfaces and amount of chiral dopants.

The diffraction efficiency  $\eta_m$  of order  $m$  for the achromatic PG also may be calculated using Jones calculus<sup>25,26</sup> under the paraxial (small-angle) approximation. Since the derivation for our anisotropy profile (Eqs. (2)) involves lengthy expressions, here we will only summarize the approach and include the final result (referring the reader

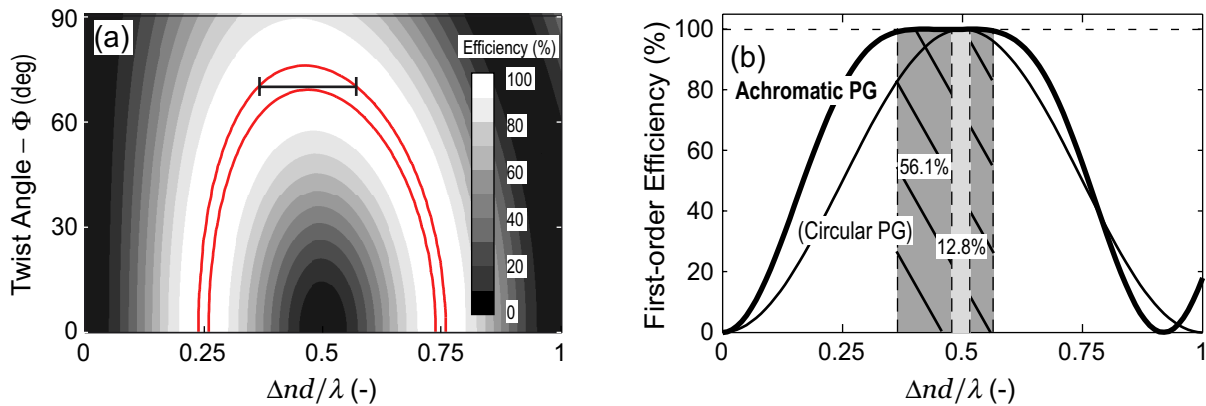


Figure 2. Expected diffraction properties of an achromatic PG from the Jones vector analysis: (a) diffraction efficiency map for different twist angles  $\Phi$  and (b) the first-order efficiency spectrum with the maximum bandwidth for high diffraction efficiencies ( $\geq 99\%$ ). Note that the maximum bandwidth can be achieved when  $\Phi \approx 70^\circ$  (highlighted in the part (a)).

to Ref.<sup>14</sup> for details). First, we find the spatially-varying  $2 \times 2$  transfer matrix  $\mathbf{T}_{APG}(x)$ , incorporating all grating geometry and material anisotropy. The achromatic PG profile is expressed as multiple thin layers of Circular PGs with a small lateral phase shift between them, akin to the analysis of twisted nematic LC modes as stratified media.<sup>27</sup> Second, we find the electric field of diffraction order  $m$  far from the grating as  $\mathbf{D}_m = (1/\Lambda) \int_0^\Lambda \mathbf{T}_{APG}(x) \mathbf{E}_{in} e^{-i2\pi mx/\Lambda} dx$ . Finally, we determine the diffraction efficiency as  $\eta_m = |\mathbf{D}_m|^2/|\mathbf{E}_{in}|^2$ , which may be analytically summarized by the following:

$$\eta_0 = [\cos^2 X + (\Phi^2 - \Gamma^2) \operatorname{sinc}^2 X]^2 \quad (3a)$$

$$\eta_{\pm 1} = \frac{A^2}{2} (1 \mp S'_3) (\cos^2 X + \Phi^2 \operatorname{sinc}^2 X) \quad (3b)$$

where  $\Gamma = \pi \Delta n d / \lambda$ ,  $X = \sqrt{\Phi^2 + \Gamma^2}$ ,  $A = 2\Gamma \operatorname{sinc} X$ , and  $\operatorname{sinc} X \equiv (\sin X)/X$ . The grating equation  $\sin \theta_m = m\lambda/\Lambda \pm \sin \theta_{in}$  governs diffraction angles (Fig. 1(a)).

Several important properties should be noted in Eqs. (3) and in Ref.<sup>14</sup> *First*, only three diffraction orders (0 and  $\pm 1$ ) exist, which depend on both the retardation  $\Delta n d / \lambda$  and the twist angle  $\Phi$ . We will show that  $\Sigma \eta_{\pm 1} \approx 100\%$  over a wide wavelength range by balancing the effect of retardation and twist. *Second*, the first-orders have orthogonal circular polarizations (Fig. 1(c)). *Third*, the first-order efficiencies are strongly sensitive to the incident polarization state through  $S'_3$  (akin to Circular PGs). *Overall*, we understand the achromaticity of the two antisymmetric chiral layers as self-compensation, via counteracting chromatic dispersions in the linear and twist-induced circular birefringences.<sup>13</sup>

To enable quantitative evaluation, we define bandwidth as  $\Delta\lambda/\lambda_0$ , the ratio of the spectral range  $\Delta\lambda$  (over which high diffraction efficiency  $\Sigma \eta_{\pm 1} \geq 99\%$  occurs) to the center wavelength  $\lambda_0$ . We employ Eq. (3b) to generate a map of total first-order diffraction efficiency as a function of the retardation and the twist angle (shown in Fig. 2(a)). The maximum bandwidth ( $\simeq 56.1\%$ ) is found when  $\Phi = 70^\circ$ . Note, this is more than a four-fold enhancement as compared with a conventional Circular PG ( $\simeq 12.8\%$ ), as shown in Fig. 2(b) with relative bandwidths highlighted.

### 3. SWITCHABLE, ACHROMATIC LCPGS ON REFLECTIVE SUBSTRATES

We introduce a simple but effective way to implement a reflective version of the achromatic PG, which allows electro-optical switching as well as the same polarization diffraction properties in principle. Use of a reflective substrate effectively captures the self-compensation of retardation dispersion within a single cell. In addition, the degenerate surface allows to control the twist angle only by the amount of chiral dopants without precision substrate registrations. We expect the same diffraction properties as expected from the Jones vector analysis in Eqs. 3. We will discuss the basic structure, fabrication methods, and experimental results of the electro-optical behaviors of reflective achromatic LCPGs in this section.

#### 3.1 Structure

The achromatic LCPG consists of a cell structure of a transmissive substrate with a LC alignment layer on a transparent electrode (i.e., ITO) and a reflective substrate (i.e., aluminum coated glass), whose surface is treated for degenerate anchoring of LCs. The cell thickness  $d$  is determined to deliver a half-wave retardation (i.e.,  $d \approx \lambda/2\Delta n$ ) when light travels through the cell. The cell is filled with nematic liquid crystals with  $\sim 70^\circ$  twist to form the grating as shown in Fig. 1(d), which is controlled by surface alignment and amount of chiral dopants in the LC mixture. Without applied fields, light over a broad range of wavelengths (450 nm to 650 nm) is diffracted into the first-orders.

Electro-optical switching can be achieved by applying an electric field across the cell and a voltage over the threshold will deform the LC profile to be tilted along the field direction. Since the LC profile will keep the same twist angle, the diffraction spectra will move up and down with varying the voltage without noticeable spectral shifts. When the applied voltage is high enough to erase the grating structure, light will be directly reflected.

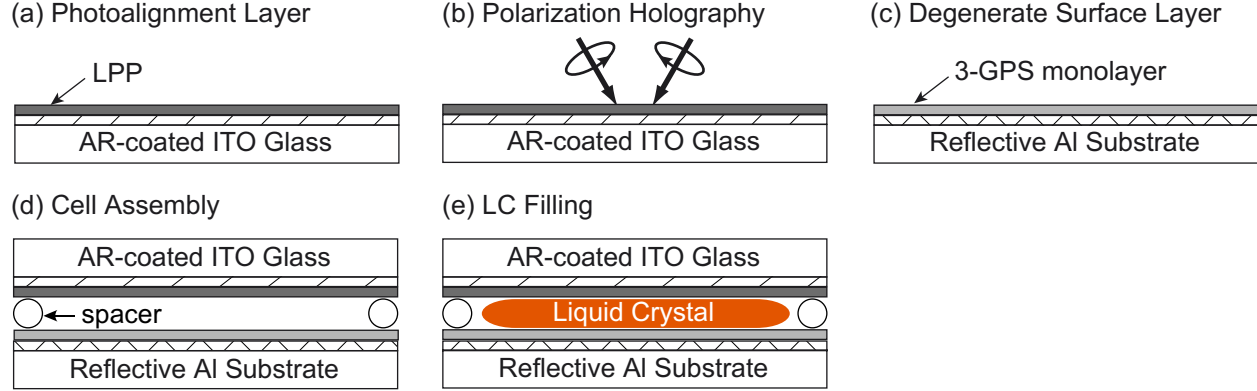


Figure 3. Fabrication procedures for reflective achromatic LCPGs using the polarization holography and photo-alignment techniques for LCs. A spiraling anisotropy profile is patterned on the photoalignment layer (LPP) surface and the reflective surface is coated with 3-GPS for degenerate anchoring of LCs. Then, both substrates are assembled to form a cell to fill with LC mixtures.

### 3.2 Fabrication

We have fabricated defect-free LCPGs (conventional Circular PGs) with ultra-high efficiency ( $\geq 99\%$ ) and low scattering ( $< 0.2\%$ ) by polarization holography and photo-alignment techniques for LCs.<sup>4,5</sup> The key of the fabrication technique is the use of photo-alignment materials that allow the separation of hologram recording and grating structure amplification.<sup>28,29</sup> For achromatic LCPGs, a reflective substrate treated for degenerate surface anchoring of LCs must be used to achieve the self-compensation effect in a single-cell structure.

As shown in Figure 3, fabrication of achromatic LCPGs proceeds with following four basic steps: first, a thin layer of photo-alignment material is coated on a ITO glass (Figure 3(a)); second, the substrate is exposed with two coherent beams from a laser with orthogonal circular polarizations at a small angle, leading to polarization interference with a constant intensity (Figure 3(b)); third, a reflective substrate with aluminum coating is prepared for its degenerate anchoring surface (Figure 3(c)); the ITO glass and reflective substrate are assembled to achieve a uniform cell thickness  $d$  and then the cell is filled with nematic LC mixtures with chiral dopants, preferably within its isotropic state (Figure 3(d)).

The following process was used for the results reported here. An index-matched ITO glass substrate (from Thin Film Devices Inc.) with a broadband AR coating was used to minimize Fresnel losses due to index mismatch (i.e., reflections at an air-glass interface). We coated the ITO substrate with a photoalignment material ROP103-2CP (from Rolic, with standard recommended coating processing). A HeCd laser (325 nm) delivering a dose of  $5 \text{ J/cm}^2$  with orthogonal circularly polarized beams was used to expose a surface periodic alignment pattern with a period of  $\Lambda = 9 \mu\text{m}$ . A standard aluminum-coated glass substrate (from Edmund Optics) was coated with (3-glycidoxypropyl) trimethoxysilane (also called 3-GPS) to form a dense, homogeneous monolayer, which allows in-plane degenerate surface anchoring of LCs. The ITO and Al substrates were assembled to form a  $3 \mu\text{m}$ -thickness cell. We prepared a LC mixture of nematic liquid crystal MLC-12100-000 (from Merck,  $\Delta n = 0.113$ ,  $T_{NI} = 92 \text{ }^\circ\text{C}$ ,  $K_1 = 11.4 \text{ pN}$ ,  $K_3 = 13.8 \text{ pN}$ ,  $\Delta\epsilon = 8.5$ ,  $\gamma_1 = 183 \text{ mPa}\cdot\text{sec}$ ) with a small amount ( $\sim 0.22\%$ ) of chiral dopant CB15 (from Merck, right-handed,  $\text{HTP} \simeq 7.3 \mu\text{m}^{-1}$ ), chosen so that the twist angle  $\Phi = 70^\circ$ . Filling of the LC mixture was done on a hotplate at  $130 \text{ }^\circ\text{C}$ .

## 4. ELECTRO-OPTICAL BEHAVIORS OF REFLECTIVE ACHROMATIC LCPGS

We have demonstrated a reflective achromatic LCPG that allows electrical switching of broadband light (i.e., white light or red, green, blue LEDs). Several definitions will be helpful as we characterize the inherent properties of achromatic LCPGs: (i) grating efficiency  $\eta_m = I_m / (I_1 + I_0 + I_{+1} + \dots)$ , is a normalized term that describes the inherent diffraction behavior, and is directly comparable to Eq. 3; (ii) total first-order reflectance  $R = (I_1 + I_{+1}) / I_{IN}$  is a true (unnormalized) measure including all substrate, interface, and grating effects; and (iii) full-on-full-off contrast ratio, defined as  $I_{ON} / I_{OFF}$ . In each of these,  $I_m$  is the measured intensity of the  $m^{\text{th}}$

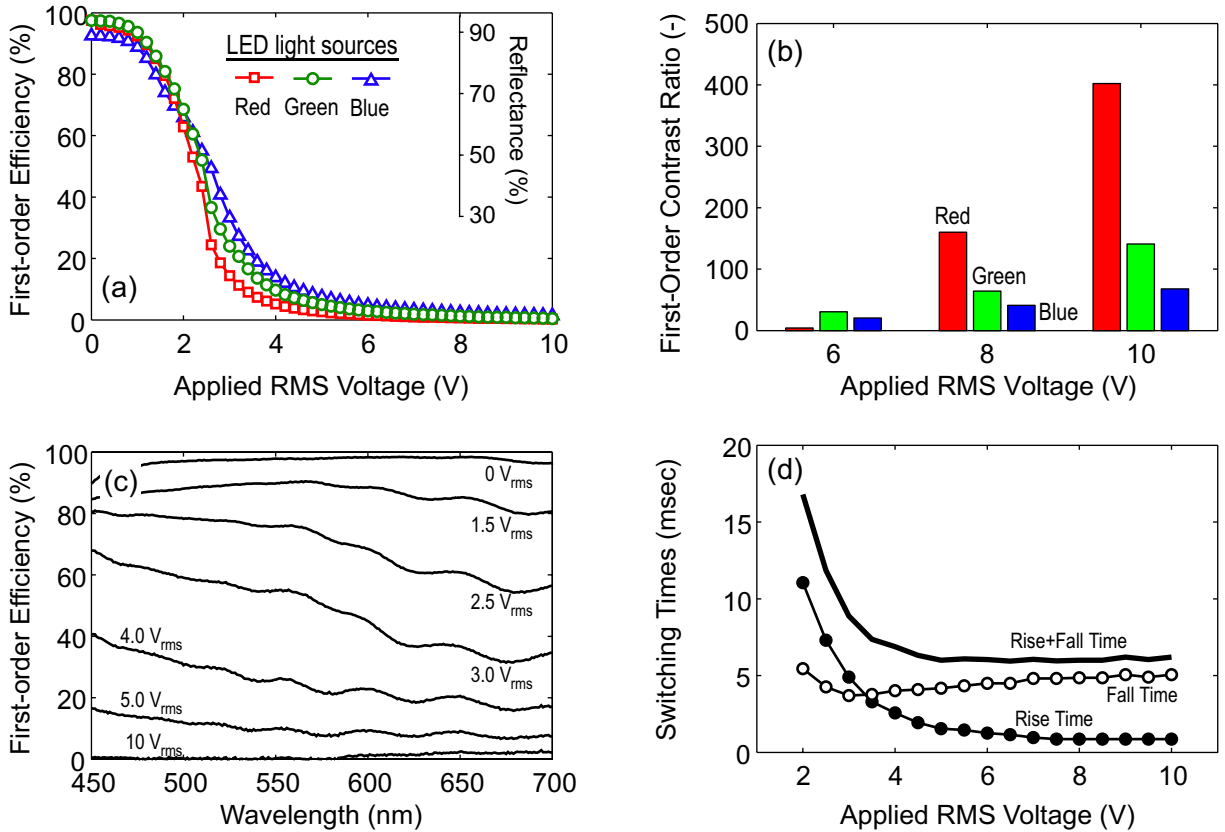


Figure 4. Electro-optical properties of the reflective achromatic LCPG sample: (a) voltage response of the first-order efficiency for RGB LED light; (b) contrast ratios at 6, 8, 10 V; (c) diffraction spectra with various applied voltages; (d) switching times.

reflected diffraction order,  $I_{IN}$  is the incident intensity, and  $I_{ON}/I_{OFF}$  is the maximum/minimum total first-order incident intensity. Electro-optic measurements on mirror-substrates involved a 4 kHz square wave (with zero DC bias). Note that all applied voltages were in RMS values.

The voltage response of a reflective LCPG ( $\Lambda = 9 \mu m$ ,  $d = 3 \mu m$ ) is shown in Fig. 4(a). The grating efficiency and reflectance (of the first-orders) were measured with unpolarized red, green, and blue LEDs (collimated for this measurement to  $\sim 4^\circ$ ). We observe that the achromatic LCPG diffracts all RGB LEDs with efficiency  $\Sigma\eta_{\pm 1} \geq 95\%$  and reflectance  $R \geq 90\%$  without voltage modulation. Diffraction efficiencies for red and green LEDs ( $\geq 98\%$ ) reach nearly the 100% theoretical value while the blue LED produces a slightly lower value ( $\sim 95\%$ ) due to the dispersion of LC birefringence (in general, larger values for shorter wavelengths). Further optimization can be done by a fine tuning of the thickness and the amount of chiral dopants in the LC mixture. Losses in reflectance predominantly result from electrode-absorptions. Note that the achromatic LCPG sample does not show a voltage threshold.

The contrast ratios were also measured by comparing first-order diffracted powers without applied voltage (0 V) with respect to diffracted powers at three different applied voltages (6, 8, 10 V). As shown in Fig. 4(b), the maximum contrast ratio  $\geq 400$  was measured with red LED light (contrast ratios of 140 and 70 with green and blue LEDs, respectively), which is much higher than the best previous report of conventional reflective LCPGs<sup>5</sup> (i.e.,  $CR \geq 50$  at 13 V applied voltage). We believe that the effect of twist and degenerate surface anchoring of LCs result in such a low voltage threshold and high contrast ratios.

To characterize the grayscale operation, we also measured diffraction spectra of the achromatic LCPG with varying applied voltages. We estimated the first-order efficiency from the zero-order reflection spectra ( $\Sigma\eta_{\pm 1} \approx \eta_0$ ) because of difficulty of its direct measurement. Fig. 4(b) shows estimated first-order efficiencies at different

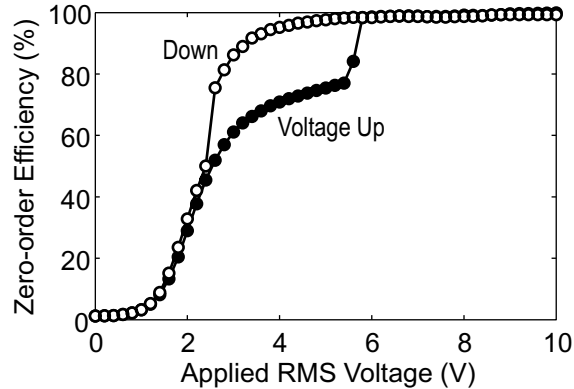


Figure 5. Voltage response of the zero-order efficiency with HeNe red laser light. A hysteresis is observed and the transitions occur at  $\sim 6$  V and  $\sim 2.5$  V while increasing and decreasing applied voltages, respectively.

RMS voltages (0, 1.5, 2.5, 3, 4, 5, 10 V). The diffraction spectrum moves mostly up-and-down without noticeable spectral shifts. In addition, the achromatic LCPG exhibits a steeper grayscale curve than the conventional LCPGs.<sup>5</sup>

The dynamic response was also characterized, where a few ms total switching times are typical for conventional LCPGs.<sup>4</sup> Fig. 5(a) shows the rise and fall times (10% – 90% transitions) of the achromatic LCPG switching from 0V to the indicated applied voltage. The total switching times  $\sim 6$  ms was measured. The general trend is similar to other LC modes: rise-time is strongly dependent on voltage, while fall-time is roughly constant. These switching times are  $\sim 2$  times faster than a conventional LCPG with a same thickness while a normal LCPG requires a 1/4-wave thickness instead of a 1/2-wave thickness. Since the switching times are generally proportional to a square of the thickness, the increase of switching times due to doubled thickness of the reflective achromatic LCPG is only two-times rather than four-times with respect to those of a conventional reflective LCPG.

Somewhat surprisingly, we noticed a hysteresis in the voltage response curve of diffraction efficiencies (both zero- and first-order) of the reflective achromatic LCPG sample, as shown in Fig. 5. We believe that such a hysteresis has its origin in the presence of twist in the LCPG cell.<sup>30,31</sup> Transitions for the hysteresis are always found at certain applied voltages across many samples as shown in Fig. 5; one transition occurs at  $\sim 6$  V while increasing the voltage and the other occurs at  $\sim 2.5$  V while decreasing the voltage. This effect appears more evident in the voltage response of the zero-order efficiency as shown in Fig. 5, while it is also seen from the first-order diffraction. We will investigate more on this interesting electro-optical properties in the future.

## 5. CONCLUSIONS

We have demonstrated an achromatic LCPG as electrically switchable reflective LC device, which manifests high efficiency ( $\geq 95\%$ ) over a broad spectral range. We stress that this polarizer-free LC device can modulate white, unpolarized light, which we demonstrate here with red, green, and blue LEDs. To achieve these achromatic properties, we employed a reflective substrate with special surface treatment using 3-GPS for in-plane degenerate anchoring of LCs. The reflective configuration allows self-compensation for achromatic diffraction within a single cell structure with aid of the chiral (or antisymmetric) nature of LC twist (flipping to the opposite handedness upon reflection). The achromatic LCPG sample shows uniform diffraction spectra with less spectral shifts in grayscale operation. We also found the presence of a noticeable hysteresis in the reflectance voltage response, which we suspect is caused in part by the twisting tendency of the chiral nematic. Relatively fast switching times ( $\sim 6$  ms) and zero threshold voltage were measured for the first-order diffraction. The achromatic LCPG offers advantages of broadband unpolarized light switching at high efficiency, reasonably high switching speed, and excellent grayscale characteristics, which are all important parameters for displays, optical communication, data storage, and many other applications.

## ACKNOWLEDGMENTS

The authors gratefully acknowledge support from the National Science Foundation (grant ECCS-0621906).

## REFERENCES

- [1] Escuti, M. J. and Jones, W. M., "Polarization independent switching with high contrast from a liquid crystal polarization grating," *SID Int. Symp. Digest Tech. Papers* **37**, 1443–1446 (2006).
- [2] Provenzano, C., Pagliusi, P., and Cipparrone, G., "Highly efficient liquid crystal based diffraction grating induced by polarization holograms at the aligning surfaces," *Appl. Phys. Lett.* **89**, 121105 (2006).
- [3] Sarkissian, H., Serak, S. V., Tabiryan, N. V., Glebov, L. B., Rotar, V., and Zeldovich, B. Y., "Polarization-controlled switching between diffraction orders in transverse-periodically aligned nematic liquid crystals," *Opt. Lett.* **31**, 2248–2250 (2006).
- [4] Komanduri, R. K., Jones, W. M., Oh, C., and Escuti, M. J., "Polarization-independent modulation for projection displays using small-period LC polarization gratings," *Journal of the SID* **15**, 589–594 (2007).
- [5] Komanduri, R. K., Oh, C., Kekas, D. J., and Escuti, M. J., "Polarization independent liquid crystal microdisplays," *SID Int. Symp. Digest Tech. Papers* **39**, 18.3 (2008).
- [6] Ren, H. W., Lin, Y. H., and Wu, S. T., "Polarization-independent and fast-response phase modulators using double-layered liquid crystal gels," *Appl. Phys. Lett.* **88**, 061123 (2006).
- [7] Drevensek-Olenik, I., Copic, M., Sousa, M. E., and Crawford, G. P., "Optical retardation of in-plane switched polymer dispersed liquid crystals," *J. Appl. Phys* **100**, 033515 (2006).
- [8] Jazbinsek, M., Olenik, I. D., Zgonik, M., Fontecchio, A. K., and Crawford, G. P., "Characterization of holographic polymer dispersed liquid crystal transmission gratings," *J. Appl. Phys* **90**, 3831–3837 (2001).
- [9] Chen, J., Bos, P. J., Vithana, H., and Johnson, D. L., "An electrooptically controlled liquid-crystal diffraction grating," *Appl. Phys. Lett.* **67**, 2588–2590 (1995).
- [10] Ferriere, R. and Goedgebuer, J. P., "Achromatic system for far-field diffraction with broadband illumination," *Appl. Opt.* **22**, 1540–1545 (1983).
- [11] Lancis, J., Minguez-Vega, G., Tajahuerce, E., Climent, V., Andres, P., and Caraquitena, J., "Chromatic compensation of broadband light diffraction: Abcd-matrix approach," *J. Opt. Soc. Am. A* **21**, 1875–1885 (2004).
- [12] Lajunen, H., Turunen, J., and Tervo, J., "Design of polarization gratings for broadband illumination," *Opt. Express*. **13**, 3055–3067 (2005).
- [13] Scheffer, T. and Nehring, J., "Super-twisted nematic (STN) liquid crystal displays," *Annu. Rev. Mater. Sci.* **27**, 555–583 (1997).
- [14] Oh, C. and Escuti, M. J., "Achromatic polarization gratings as highly efficient thin-film polarizing beam-splitters for broadband light," *Proc. SPIE* **6682**, 668211 (2007).
- [15] Oh, C. and Escuti, M. J., "Achromatic polarization gratings as highly efficient thin-film polarizing beam-splitters for broadband light," *Opt. Lett.*, accepted for publication (2008).
- [16] Nikolova, L. and Todorov, T., "Diffraction efficiency and selectivity of polarization holographic recording," *Opt. Acta* **31**, 579–588 (1984).
- [17] Huang, T. and Wagner, K., "Coupled mode analysis of polarization volume hologram," *IEEE Journal of Quantum Electronics* **31**, 372–390 (1995).
- [18] Gori, F., "Measuring stokes parameters by means of a polarization grating," *Opt. Lett.* **24**, 584–586 (1999).
- [19] Tervo, J. and Turunen, J., "Paraxial-domain diffractive elements with 100% efficiency based on polarization gratings," *Opt. Lett.* **25**, 785–786 (2000).
- [20] Oh, C. and Escuti, M. J., "Numerical analysis of polarization gratings using the finite-difference time-domain method," *Phys. Rev. A* **76**, 043815 (2007).
- [21] Escuti, M. J., Oh, C., Sanchez, C., Bastiaansen, C. W. M., and Broer, D. J., "Simplified spectropolarimetry using reactive mesogen polarization gratings," *Proc. SPIE* **6302**, 632614 (2006).
- [22] Collett, E., *Polarized Light: fundamentals and applications* (Marcel Dekker, 1993).
- [23] Broer, D. J., "Insitu photopolymerization of oriented liquid-crystalline acrylates .3. oriented polymer networks from a mesogenic diacrylate," *Macromol. Chem. Phys.* **190**, 2255–2268 (1989).

- [24] Kelly, S. M., "Anisotropic networks," *J. Mater. Chem.* **5**, 2047–2061 (1995).
- [25] Jones, R. C., "A new calculus for the treatment of optical systems. i. description and discussion of the calculus," *J. Opt. Soc. Am.* **31**, 488–493 (1941).
- [26] van Heesch, C., "Polarization-selective diffraction for display applications," *Ph.D. Dissertation*, Eindhoven University of Technology, Eindhoven, Netherlands (2007).
- [27] P. Yeh and C. Gu, *Optics of Liquid Crystal Displays* (Wiley, 1999).
- [28] Crawford, G. P., Eakin, J. N., Radcliffe, M. D., Callan-Jones, A., and Pelcovits, R. A., "Liquid-crystal diffraction gratings using polarization holography alignment techniques," *J. Appl. Phys.* **98**, 123102 (2005).
- [29] Provenzano, C., Cipparrone, G., and Mazzulla, A., "Photopolarimeter based on two gratings recorded in thin organic films," *Appl. Opt.* **45**, 3929–3934 (2006).
- [30] Bauer, M., Boeffel, C., Kuschel, F., and Zschke, H., "Evaluation of chiral dopants for LCD applications," *Journal of SID* **14**, 805–812 (2006).
- [31] Liang, B. and Lin, C. L., "Crucial influence on d/p range in bistable chiral tilted-homeotropic nematic liquid crystal cells," *J. Appl. Phys.* **102**, 124504 (2007).